Acta Crystallographica Section D
Biological Crystallography
ISSN 0907-4449

Effects of the silanized mica surface on protein crystallization

L. Tang,[a] Y. B. Huang,[a] D. Q. Liu,[a] J. L. Li,[a] K. Mao,[a] L. Liu,[b] Z. J. Cheng,[b] W. M. Gong,[b,c] J. Hu[a,d] and J. H. He[a]*

[a]Shanghai Institute of Applied Physics, Chinese Academy of Sciences, 2019 Baojia Road, Shanghai 201800, People's Republic of China, [b]Key Laboratory of Structural Biology of the Chinese Academy of Sciences, School of Life Sciences, University of Science and Technology of China, Hefei 230026, People's Republic of China, [c]Institute of Biophysics, Chinese Academy of Sciences, 15 Datun Road, Beijing 100101, People's Republic of China, and [d]Nanobiology Laboratory of Bio-X Life Science Research Center, Shanghai JiaoTong University, 1954 Huashan Road, Shanghai 200030, People's Republic of China

Correspondence e-mail: hejh@ssrc.ac.cn

Received 3 June 2004
Accepted 14 October 2004

A freshly cleaved mica surface silanized by 3-aminopropyl triethoxysilane is flat over a large area, displays a controlled degree of hydrophobicity and contains positive charges. In this paper, mica sheets silanized by this method have been used as crystallization surfaces for lysozyme, trichosanthin and three other proteins of unknown structure. Crystallization experiments have been carried out by the hanging-drop vapour-diffusion technique and the results indicate that the silanized mica surface can ameliorate the protein crystallization process considerably compared with a silanized glass cover slip control. For lysozyme on the silanized mica surface, the induction time required for crystal growth decreases markedly. For trichosanthin, the crystal size is obviously larger and the number of crystals grown is much lower. For the three proteins of unknown structure, the diffraction ability of the crystals is improved considerably.

1. Introduction

The functions of proteins are dependent on their three-dimensional structure and the most powerful technique for determining protein structures is X-ray crystallography (see statistics from the Protein Data Bank at http://www.rcsb.org), which requires well ordered crystals. Nowadays, the production of crystals suitable for X-ray crystallography is found to be the bottleneck in the protein structure-determination process. This fact is becoming more and more obvious from pilot structural genomics projects, which show that the success rate of moving from clone to structure is about 10% (http://proteome.bnl.gov/progress.html). Many efforts have been made by different laboratories to improve the process of protein crystallization and the effects of magnetic fields (Maki *et al.*, 2004; Lin *et al.*, 2000), electric fields (Nanev & Penkova, 2001), microgravity (DeLucas *et al.*, 1989, 2002), pH, ionic strength and temperature on crystallization have been investigated extensively (Baird *et al.*, 2001; Kuznetsov *et al.*, 2001; Kitano *et al.*, 1998; Lorber & Giegé, 1992; Nadarajah *et al.*, 1995). At the same time, in order to obtain high-quality protein single crystals, various materials have been tested as crystallization surfaces, for instance, mineral surfaces (McPherson & Shlichta, 1988; Kimble *et al.*, 1998), lipid layers (Edwards *et al.*, 1994), porous silicon (Chayen *et al.*, 2001), poly-L-lysine (Fermani *et al.*, 2001), chemically modified mica surfaces (Falini *et al.*, 2002) and poly(vinylidene fluoride) (Punzi *et al.*, 1991; Chayen & Saridakis, 2001). It has been demonstrated that for individual proteins some material surfaces can promote protein nucleation and some can relax the crystallization conditions required for crystal growth. However, no surface has shown general effectiveness that can be widely used in protein crystallization.

If crystals are to be suitable for X-ray diffraction they should be of good quality and reasonably large size. Therefore, surfaces that promote protein nucleation, suppress the number of crystals formed and facilitate the growth of large crystals will be preferred for protein crystallization.

Mica is a natural mineral characterized by a layered structure. This feature allows the cleavage of the mineral along the basal plane (001) to form thin, rigid and smooth sheets, which are widely used as flat reference surfaces at the atomic level (Nishimura *et al.*, 1994). A freshly cleaved mica surface silanized by 3-aminopropyl triethoxysilane *via* a special technique (Huang *et al.*, 2000), named APTES-mica, has been developed for the nanomanipulation of DNA (Hu *et al.*, 2002) by atomic force microscopy (AFM). Since this surface is flat over a large area (usually over tens of square micrometres), displays a controlled degree of hydrophobicity and contains positive charges, it is expected to be suitable for protein crystal growth. In the present paper, we have used APTES-mica sheets as crystallization surfaces for several proteins. Experimental results for hen egg-white lysozyme (HEWL) and trichosanthin have shown several advantages of the use of APTES-mica over the use of conventional silanized glass cover slips (SGCS), namely a shorter induction time, a larger crystal size and a smaller number of crystals. APTES-mica has also been used in the crystallization of three proteins, a coactosin-like protein (K115), homoserine *O*-acetyltransferase (Hoat) and a thioesterase-like protein (K169), the structures of which are unknown. High-quality crystals were rarely obtained using SGCS despite years of effort. Our experimental results have shown that using APTES-mica as a crystallization surface can considerably ameliorate the crystallization process and lead to the production of high-quality crystals.

2. Materials and methods

2.1. Materials

HEWL was purchased from the Sigma Chemical Co. Trichosanthin was a gift from Professor Xia Zhongxiang. K115, Hoat and K169 were purified in our laboratory. 3-Aminopropyl triethoxysilane (APTES), used to silanize the mica, was purchased from the Sigma Chemical Co. Mica (muscovite) was purchased from the Sichuan Yaan Mica Company. Silanized glass cover slips (SGCSs) were purchased from the Shanghai Shengzheng Biotechnology Company. Plastic slips were purchased from Fisher Scientific International. The digital camera is a commercial product from Olympus.

2.2. Preparation of mica surface

The freshly cleaved mica surface was washed with 100 m*M* nickel nitrate and pure water and a drop of an aqueous solution of 1%(*v*/*v*) APTES with a dosage of about 1 µl cm^{-2} was then deposited on the surface. 5 min later, the surface was washed with pure water and then heated in an oven at 393 K for several hours. The hydrophobic property of APTES-mica was roughly in proportion to the heating time. In our experiments, the heating time was 2–3 h. APTES-mica was then cut into small sheets and stored in a desiccator. The APTES-mica treatment technique was initially described by Hu *et al.* (1996) and subsequently, with improvements, by Huang *et al.* (2000).

Table 1
The crystallization starting conditions.

Protein	Molecular weight (kDa)	Protein concentration (mg ml^{-1})	Reservoir solution
HEWL	14	50	6.4, 5.8, 2.8%(*w*/*v*) sodium chloride, 0.08, 0.06, 0.035 *M* sodium acetate pH 4.8
Trichosanthin	27	40	0.075 *M* citric acid buffer solution, 14%(*w*/*v*) potassium chloride pH 5.4
K115	16	25	22%(*v*/*v*) PEG 2000, 0.1 *M* MES pH 6.5
Hoat	38	20	9%(*v*/*v*) PEG 20 000, 0.1 *M* MES, pH 6.5
K169	16	20	20%(*v*/*v*) PEG MME 2000, 0.1 *M* acetate buffer solution, 150 m*M* ammonium sulfate pH 4.2

2.3. Crystallization experiments

Crystallization trials on HEWL and trichosanthin were carried out at room temperature by the hanging-drop vapour-diffusion technique with a 16-well tissue-culture tray and the crystallization trials on K115, Hoat and K169 were carried out at 277 K with a 24-well tissue-culture tray. The starting conditions of crystallization are shown in Table 1.

An aliquot of protein was mixed with an equal volume of reservoir solution in a hanging drop on APTES-mica or the SGCS. The hanging drop was then equilibrated against the reservoir solution in the tissue-culture tray. The cover slip was sealed to the tray well with vaseline. The progress of the experiment was recorded using a digital camera. For HEWL, a set of successive experiments were performed by lowering the reservoir solution concentration to examine the time difference of crystallization on the APTES-mica surface and the SGCS control. To improve the statistics and reliability, each experiment using the same 12 samples was repeated at least three times.

2.4. X-ray crystal diffraction experiment

For each protein, about five to eight crystals grown on APTES-mica were screened by X-ray diffraction and more crystals grown on SGCS were screened. The diffraction data were collected by taking oscillation photographs with an oscillation angle of 0.5° using an in-house Rigaku R-AXIS IV^{++} apparatus and Cu $K\alpha$ radiation (wavelength 1.5418 Å) focused with a confocal mirror or by using the 3W1A beamline at the Beijing Synchrotron Radiation Facility. The crystal was mounted in a nylon loop and flash-cooled in a cold gaseous stream of N_2 (93 K). The cryoprotectants for K115, Hoat and K169 are shown in Table 2.

Table 2
Cryoprotectants used in X-ray crystal diffraction experiments.

K115	30%(*v*/*v*) PEG 2000, 0.1 *M* MES pH 6.5
Hoat	20%(*v*/*v*) PEG 8000, 10%(*v*/*v*) glycerol, 0.1 *M* MES pH 6.5
K169	40%(*v*/*v*) PEG MME 2000, 20%(*v*/*v*) glycerol, 0.1 *M* acetate buffer solution, 150 m*M* ammonium sulfate pH 4.2

3. Results

3.1. Effect on crystal growth speed

Observation of the crystal growth on APTES-mica and SGCS indicated that under the same conditions the induction time of HEWL crystal grown on APTES-mica was obviously reduced. To compare the growth rates under different conditions, a series of experiments were performed with different reservoir-solution concentrations, with consistent results. For example, when the reservoir-solution concentration was 6.4%(*w*/*v*) sodium chloride and 0.08 *M* sodium acetate pH 4.8, protein crystals were observed on APTES-mica 12 h after the start of the experiment, while no crystals were observed on the SGCS control. Large crystals were observed on both APTES-mica and SGCS 22 h later (Fig. 1). In another experiment, when the reservoir solution concentration was reduced to 5.8%(*w*/*v*) sodium chloride and 0.06 *M* sodium acetate pH 4.8, protein crystals began to appear on APTES-mica after 24 h, but crystals did not appear on the SGCS control until 4 d later (Fig. 2). In the third experiment, when the reservoir solution concentration was reduced to 2.8%(*w*/*v*) sodium chloride and 0.035 *M* sodium acetate pH 4.8, large protein crystals still appeared on APTES-mica after 20 d, while no crystals were observed on the SGCS control even after 28 d (Fig. 3).

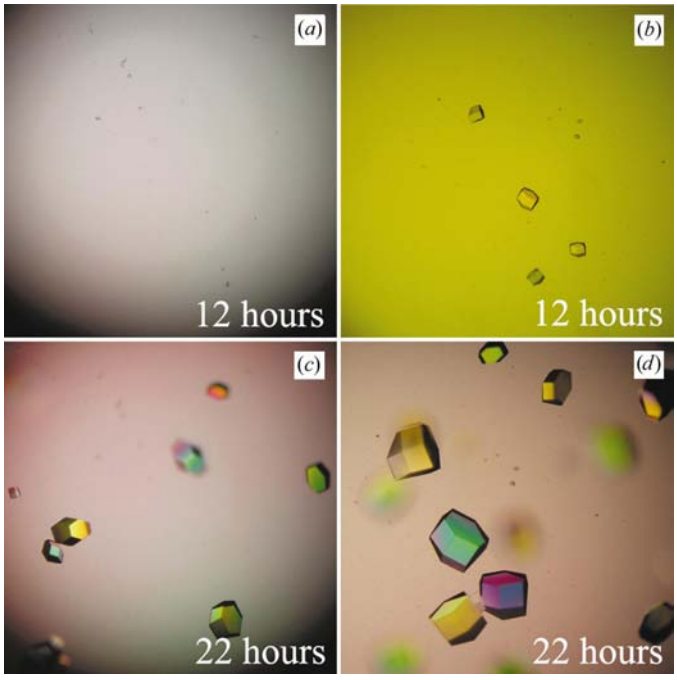

Figure 1
Microphotographs of HEWL crystals grown on SGCS (*a*, *c*) and APTES-mica (*b*, *d*) at 50 mg ml^{-1} HEWL, 6.4%(*w*/*v*) NaCl, 0.08 *M* CH_3COONa pH 4.8. HEWL crystals were observed on APTES-mica after 12 h (*b*), while nothing could be observed on the SGCS (*a*). After 22 h, HEWL crystals could be seen on both substrates (*c*, *d*). Photographs (*a*), (*b*), (*c*) and (*d*) have the same magnification.

3.2. Effect on crystal size and number

The controlled experiments using trichosanthin indicated that under the same conditions the size of protein crystals grown on APTES-mica was obviously larger than that of crystals grown on SGCS and the number of crystals was much lower. In spite of their different size and number, the crystals were of similar morphology (Fig. 4).

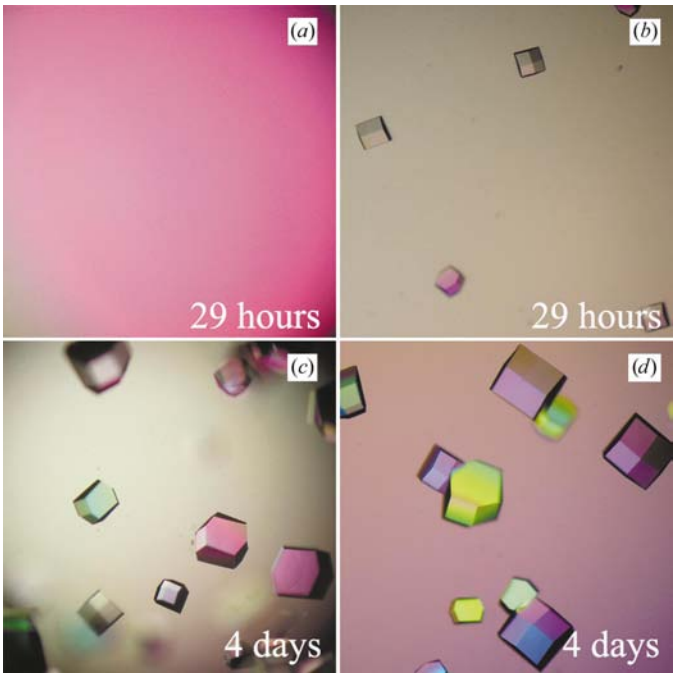

Figure 2
Microphotographs of HEWL crystals grown on SGCS (*a*, *c*) and APTES-mica (*b*, *d*) at 50 mg ml^{-1} HEWL, 5.8%(*w*/*v*) NaCl, 0.06 *M* CH_3COONa pH 4.8. HEWL crystals appeared on APTES-mica after 29 h, while no crystals appeared on the SGCS control until 4 d later. Photographs (*a*), (*b*), (*c*) and (*d*) have the same magnification.

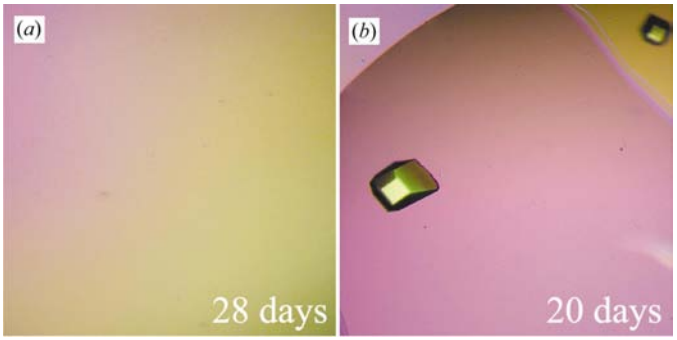

Figure 3
Microphotographs of HEWL crystals grown on SGCS (*a*) and APTES-mica (*b*) at 50 mg ml^{-1} lysozyme, 2.8%(*w*/*v*) NaCl, 0.035 *M* CH_3COONa pH 4.8. HEWL crystals began to appear on APTES-mica after 20 d, while no crystals were observed on the SGCS control even after 28 d. The two photographs have the same magnification.

3.3. Effect on crystal quality

For HEWL and trichosanthin, all the crystals screened diffracted very well, whether they were grown on APTES-mica or SGCS. Diffraction ability is not a sensitive test of crystal quality.

However, the experiments on the proteins K115, Hoat and K169, the structures of which are still unknown, indicated that using APTES-mica sheets as crystallization surfaces promoted the formation of high-quality protein crystals. On SGCS, K115, Hoat and K169 were prone to form crystals with malformed appearance and weak diffraction ability that were unsuitable for X-ray diffraction experiments. Those crystals grown on SGCS had poor diffraction ability and their diffraction resolution was no better than 3.5 Å, even though synchrotron radiation was used. However, high-quality crystals could be obtained easily when APTES-mica was used as a crystallization surface for these three proteins. These crystals not only had good shape and low anisotropy (Fig. 5), but also had good diffraction ability. The best diffraction resolutions that we obtained on an in-house X-ray machine were 2.0 Å for K115, 2.4 Å for Hoat and 3.0 Å for K169. Fluctuation of diffraction resolution exists for different crystals of each protein grown under the same conditions, but is reasonably small compared with the difference between the crystals grown on APTES-mica and on SGCS. For example, most of the crystals of K115 diffract to 2.5 Å resolution, which is much better than all the K115 crystals grown on SGCS. The best diffraction photographs obtained for these three proteins are shown in Fig. 6. For K115, Hoat and K169 crystals grown on SGCS, diffraction spots are very sparse (Figs. 6*d*, 6*e* and 6*f*) and the diffraction resolution is also much lower than that of the crystals grown on APTES-mica (Figs. 6*a*, 6*b* and 6*c*). The indexing indicated that the crystals grown on APTES-mica and the SGCS belonged to the same space group, although they had obviously different diffraction ability. For example, all K115 crystals, whether grown on APTES-mica or SGCS, belong to space group $P2_12_12_1$ with the same unit-cell parameters: $a = 28.03$, $b = 55.38$, $c = 70.79$ Å. This is the case for all three proteins.

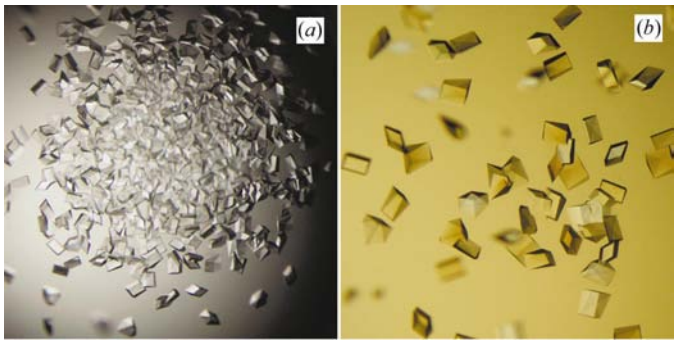

Figure 4
Microphotographs of trichosanthin crystals grown on SGCS (*a*) and APTES-mica (*b*) at 0.075 *M* citric acid buffer solution, 14%(*w*/*v*) potassium chloride pH 5.4. The size of the protein crystals grown on APTES-mica was obviously larger than that of crystals grown on the SGCS control and the number of crystals was much lower. The two photographs have the same magnification.

4. Discussion

A major problem in macromolecular crystallization is that because of excess nucleation, thousands of tiny crystals are formed in a crystallization trial instead of the desired few large crystals. It has been reported that material with a rough surface can trap protein molecules and encourage them to nucleate and form crystals (Chayen *et al.*, 2001; Chayen & Saridakis, 2001). Studies using atomic force microscopy indicate that compared with plastic cover slips and SGCS, which are often used in protein crystallization experiments, APTES-mica has a much flatter surface. It can be seen from Fig. 7 that the roughness of the APTES-mica surface is less than 0.05 nm (in undulation) within 3 μm^2, while the plastic cover slip and SGCS surfaces have many lacunae. One possible explanation is that the flat APTES-mica surface may suppress the heterogeneous nucleation of the protein and thereby effectively reduce the number of protein crystals. In order to examine further the effect of flat surfaces on crystallization, we tried to grow crystals on freshly cleaved but untreated mica surfaces, without success. Because of the strong hydrophilicity of the untreated mica surface, we failed to find a good way to contain the spread of the liquid drop on the hydrophilic mica surface without contaminating the crystallization process.

In the crystallization experiments using trichosanthin, the crystals grown on APTES-mica were of larger size and fewer in number than those grown on the SGCS control, as shown in Fig. 4. Although the size and number of crystals were distinctly different, their morphologies were similar. The X-ray diffraction experimental data indicated that all these crystals belonged to the same space group, $P2_12_12_1$, with the same unit-cell parameters, $a = 38.03$, $b = 75.54$, $c = 78.87$ Å. This result indicates that the APTES-mica surface did not change the crystal lattice.

In general, the crystal growth speed is in direct proportion to the speed of the vapour diffusion and the vapour-diffusion speed is

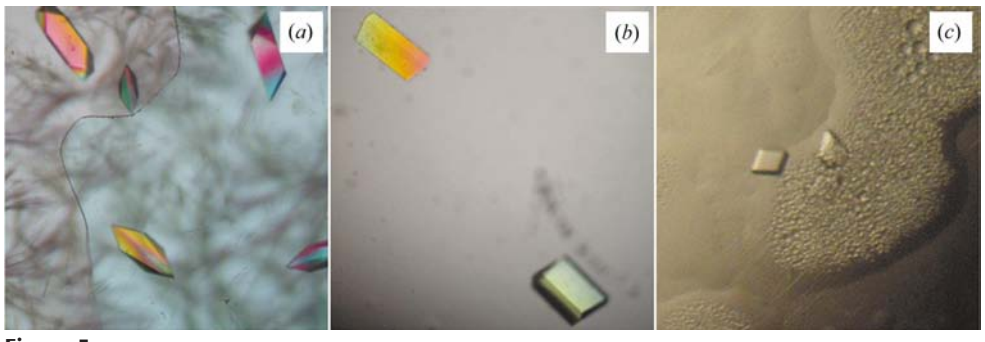

Figure 5
Microphotographs of (*a*) K115, (*b*) Hoat and (*c*) K169 protein crystals grown on APTES-mica. From the images it can be seen that these crystals have both good shape and low anisotropy.

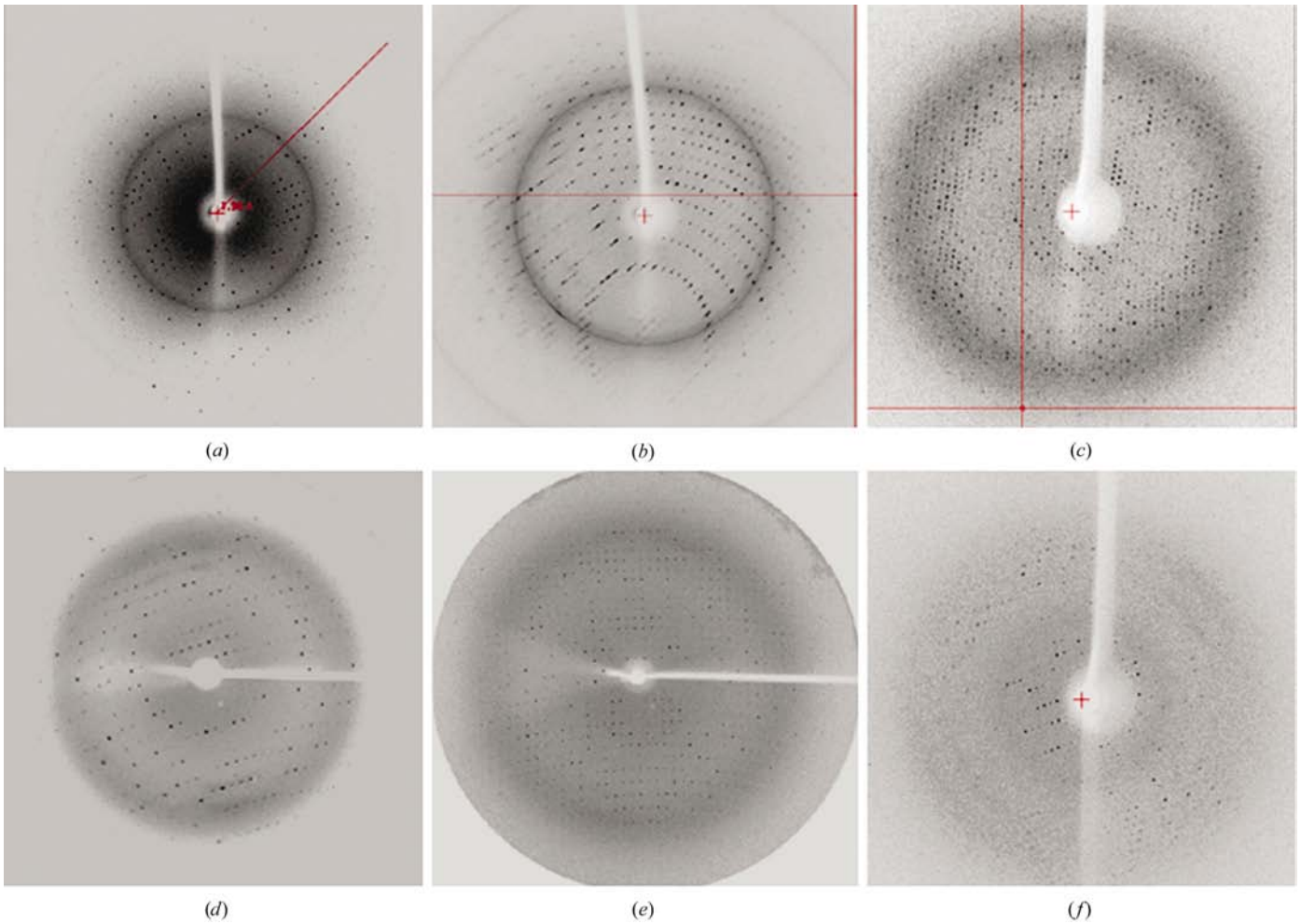

Figure 6
Oscillation photographs of (*a*) K115, (*b*) Hoat and (*c*) K169 protein crystals grown on APTES-mica and (*d*) K115, (*e*) Hoat and (*f*) K169 protein crystals grown using SGCS control. (*a*), (*b*), (*c*) and (*f*) were obtained using an in-house Rigaku R-AXIS IV^{++} apparatus and Cu $K\alpha$ radiation. (*d*) and (*e*) were obtained synchrotron radiation.

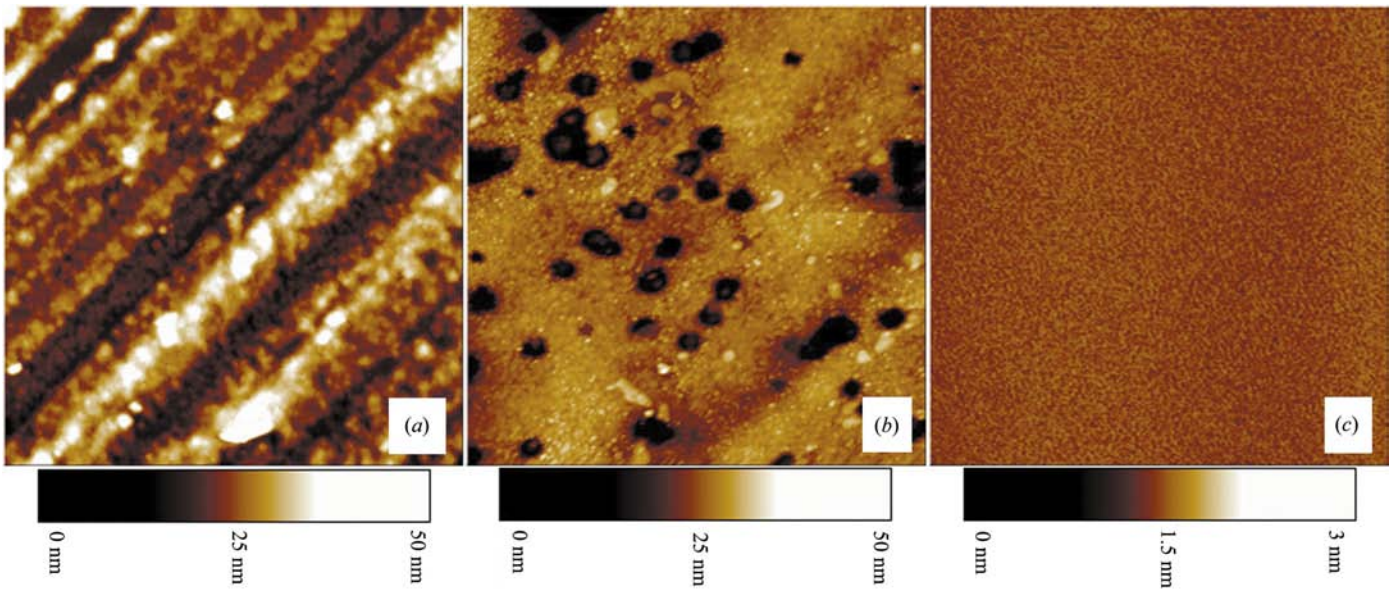

Figure 7
Images of the SGCS control (*a*), a plastic slip (*b*) and APTES-mica (*c*) by atomic force microscopy in air (Nanoscope IIIa, Digital Instruments, Santa Barbara, CA, USA, equipped with a 130 × 130 µm scanner). All the images are 3 × 3 µm in size.

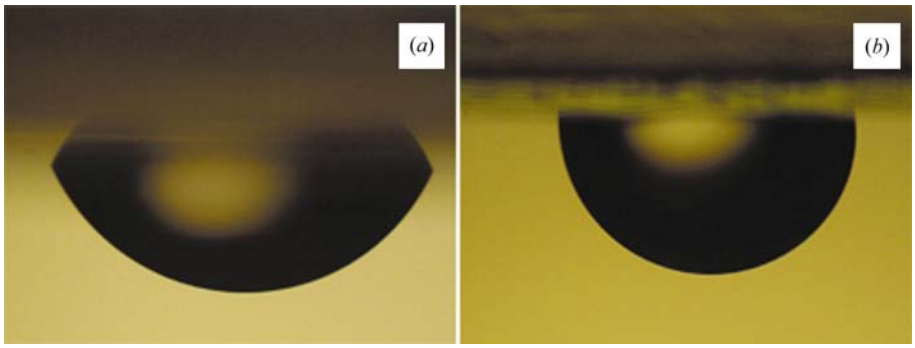

Figure 8
Photographs of the shape of liquid drops on APTES-mica (*a*) and the SGCS control (*b*) taken by a digital camera. Each drop is 2 µl in volume and the two images have the same magnification.

proportional to the surface area of the hanging drop. The hydrophobic property of the APTES-mica used in our experiments was controllable and could be adjusted according to the need of the experiments. Because the hydrophobic property of the APTES-mica used with HEWL was weaker than that of the SGCS control, the surface area of an equal volume of liquid on APTES-mica was larger than that on the SGCS, as indicated in Fig. 8. This fact may explain why the crystallization process on ATPES-mica was faster than that on the SGCS. Speeding up the crystallization process will generally cause a deterioration in the crystal quality, but in our experiments the quality of the HEWL crystals grown on APTES-mica remained the same as those grown on the SGCS control, as observed by optical microscopy. On the other hand, the crystal size tends to become small when the number of crystals increases. It is possible that the crystals grown on the SGCS might exist but were too small to be observed in our experiments, as the magnification of the optical microscope we used is only 90×. Our observation that the protein crystals appeared earlier on APTES-mica than on the SGCS control might also be partly because of this reason.

The advantages of protein crystallization on APTES-mica are more obvious for the three proteins from genes derived from human haematopoietic stem cells. Although several years of effort had been devoted to the crystallization of these three proteins, no high-quality single crystals suitable for X-ray diffraction could be obtained using SGCS. However, on APTES-mica high-quality crystals could be obtained easily under the same conditions. The obvious difference between crystals grown on APTES-mica and SGCS could not be explained by fluctuations in crystal quality. The surface roughness may have played an important role in the difference, as discussed above. The electrostatic force between APTES-mica and the protein molecules may also have contributed. The experiments on the poly-L-lysine-modified surface revealed that the number of protein crystals could be reduced by the repulsive electrostatic force between surface and protein molecules (Rong *et al.*, 2002). The proteins in our experiments carry positive charges under the experimental conditions and APTES-mica also carries positive charges as a result of its amino groups. Electrostatic repulsion could suppress the heterogeneous nucleation of the protein on APTES-mica, which may help to form fewer larger protein crystals than are grown on the SGCS control. In our other experiments, two proteins, which both carry negative charges under the crystallization conditions, were crystallized on APTES-mica, but the crystals did not show obvious improvement compared with those on the SGCS. This result conforms to our assumption. It appears that further studies are needed to better understand the crystallization on APTES-mica and the function of other characteristics of APTES-mica, such as weaker hydrophobicity and different amounts of charge.

5. Conclusion

In the present paper a unique compound, APTES-mica, has been tested as an aide to protein crystallization. APTES-mica is largely flat, displays a controlled degree of hydrophobicity and contains positive charges. By employing APTES-mica, crystal-growth time was markedly reduced and crystal size increased considerably. For specific proteins that did not yield high-quality crystals on SGCSs, APTES-mica was shown to be suitable for the growth of excellent crystalline samples. APTES-mica may yield new possibilities for the improvement of protein crystallization processes.

The authors thank Professor Ding Jianping and Dr Yu Yadong for their help with the X-ray diffraction experiments and Professor Xia Zhongxiang for providing a sample of trichosanthin. Funding from the Shanghai Institute of Applied Physics, Chinese Academy of Sciences is gratefully acknowledged.

References

Baird, J. K., Scott, S. C. & Kim, Y. W. (2001). *J. Cryst. Growth*, **232**, 50–62.
Chayen, N. E. & Saridakis, E. (2001). *J. Cryst. Growth*, **232**, 262–264.
Chayen, N. E., Saridakis, E., El-Bahar, R. & Nemirovsky, Y. (2001). *J. Mol. Biol.* **312**, 591–595.
DeLucas, L. J., Moore, K. M., Long, M. M., Rouleau, R., Bray, T., Crysel, W. & Weise, L. (2002). *J. Cryst. Growth*, **237–239**, 1646–1650.
DeLucas, L. J., Smith, C. D., Smith, H. W., Vijay-Kumar, S., Senadhi, S. E., Ealick, S. E., Carter, D. C., Snyder, R. S., Weber, P. C. & Salemme, F. R. (1989). *Science*, **246**, 651–654.
Edwards, A. M., Darst, S. A., Hemming, S. A., Li, Y. & Kornberg, R. D. (1994). *Nature Struct. Biol.* **1**, 195–197.
Falini, G., Fermani, S., Conforti, G. & Ripamonti, A. (2002). *Acta Cryst.* D**58**, 1649–1652.
Fermani, S., Falini, G., Minnucci, M. & Ripamonti, A. (2001). *J. Cryst. Growth*, **224**, 327–334.
Hu, J., Wang, M., Weier, H.-U. G., Frantz, P., Kolbe, W., Ogletree, D. F. & Salmeron, M. (1996). *Langmuir*, **12**, 1697–1700.

Hu, J., Zhang, Y., Gao, H. B., Li, M. Q. & Hartmann, U. (2002). *Nano Lett.* **2**, 55–57.
Huang, Y. B., Zhang, Y., Hu, J. & Li, M. Q. (2000). *Micrometer/Nanometer Sci. Technol.* **5**, 412–414.
Kimble, W. L., Paxton, T. E., Rousseau, R. W. & Sambanis, A. (1998). *J. Cryst. Growth*, **187**, 268–276.
Kitano, K., Motohashi, K., Yoshida, M. & Miki, K. (1998). *J. Cryst. Growth*, **186**, 456–460.
Kuznetsov, Yu. G., Malkin, A. J. & McPherson, A. (2001). *J. Cryst. Growth*, **232**, 114–118.
Lin, S.-X., Zhou, M., Azzi, A., Xu, G.-J., Wakayama, N. I. & Ataka, M. (2000). *Biochem. Biophys. Res. Commun.* **275**, 274–278.
Lorber, B. & Giegé, R. (1992). *J. Cryst. Growth*, **122**, 168–175.
McPherson, A. & Shlichta, P. (1988). *Science*, **230**, 385–387.
Maki, S., Oda, Y. & Ataka, M. (2004). *J. Cryst. Growth*, **261**, 557–565.
Nadarajah, A., Forsythe, E. L. & Pusey, M. L. (1995). *J. Cryst. Growth*, **151**, 163–172.
Nanev, C. N. & Penkova, A. (2001). *J. Cryst. Growth*, **232**, 285–293.
Nishimura, S., Biggs, S., Scales, P. J., Healy, T. W., Tsunematsu, K. & Tateyama, T. (1994). *Langmuir*, **10**, 4554–4559.
Punzi, J. S., Luft, J. & Cody, V. (1991). *J. Appl. Cryst.* **24**, 406–408.
Rong, L., Komatsu, H. & Yoda, S. (2002). *J. Cryst. Growth*, **235**, 489–493.